

REVIEW PAPER

The excitation of ionospheric convection

M. LOCKWOOD*

Rutherford Appleton Laboratory, Chilton, Didcot OX11 0QX, U.K.

(Received in final form 30 August 1990)

Abstract—This review presents recent observations of high-latitude ionospheric plasma convection, obtained using the EISCAT radar in the 'Polar' experiment mode. The paper is divided into two main parts. Firstly, the delay in the response of dayside high-latitude flows to changes in the interplanetary magnetic field is discussed. The results show the importance for the excitation of dayside convection of the transfer of magnetic flux from the dayside into the tail lobe. Consequently, ionospheric convection should be thought of as the sum of two intrinsically time-dependent flow patterns. The first of these patterns is directly driven by solar wind-magnetosphere coupling, dominates ionospheric flows on the dayside, is associated with an expanding polar cap area and is the *F*-region flow equivalent of the DP-2 *E*-region current system. The second of the two patterns is driven by the release of energy stored in the geomagnetic tail, dominates ionospheric flows on the nightside, is associated with a contracting polar cap and is equivalent to the DP-1, or substorm, current system. In the second half of the paper, various transient flow bursts observed in the vicinity of the dayside cusp are studied. These radar data, combined with simultaneous optical observations of transient dayside aurorae, strongly suggest that momentum is transferred across the magnetopause and into the ionosphere in a series of bursts, each associated with voltages of 30–80 kV. Similarities between these bursts and flux transfer events observed at the magnetopause are discussed.

1. INTRODUCTION

An understanding of how ionospheric convection is excited is of vital importance to the study of the terrestrial plasma environment and its interaction with the interplanetary medium. The control that the interplanetary magnetic field (IMF) is known to exert on the size, strength and form of the convection pattern is thought to demonstrate the dominant role of magnetic reconnection in exciting these flows [see reviews by COWLEY (1984) and REIFF and LUHMANN (1986)]. In particular, the role of the B_z (North–South) component of the IMF in controlling the number of convection cells and the transpolar voltage, and of the B_y component in generating dawn–dusk asymmetries, has led to descriptions of the ionospheric flow in terms of the prevailing B_z and B_y (HEELIS, 1984; FRIIS-CHRISTENSEN *et al.*, 1985; HEPPNER and MAYNARD, 1987). Implicit in such descriptions is the assumption that the ionospheric flow pattern rapidly adjusts to the prevailing IMF and does not depend upon the previous history of the IMF orientation. However, the IMF generally does not maintain the same orientation for more than 2 h: from a survey of 9 months of 15-s IMF data, ROSTOKER *et al.* (1988) found that

this was the case for only 15.4% of the time. From hourly averages of IMF data, HAPGOOD *et al.* (1991) found that this figure varied between 10 and 40% over a 24-yr period, with some suggestion of a solar cycle variation. A period of 2 h is taken to be significant because CLAUSER *et al.* (1981) found this to be the magnetospheric impulse response time from studies of geomagnetic disturbance; BARGATZE *et al.* (1985) found a somewhat lower time of 1 h. Furthermore, HOLZER *et al.* (1986) have shown, using precipitation data from two polar orbiting spacecraft, that the polar cap area oscillates with a period of a few hours following a southward turning of the IMF. Therefore, for the majority of the time, the IMF is varying on time scales shorter than the magnetospheric response time and the assumption that convection is in equilibrium with the prevailing IMF may well be inadequate.

Reconnection at the dayside magnetopause is thought to take place in either a quasi-steady manner or in a series of bursts, termed 'flux transfer events' (FTEs) (RUSSELL and ELPHIC, 1978, 1979; PASCHMANN *et al.*, 1982, 1986; SAUNDERS *et al.*, 1984; FARRUGIA *et al.*, 1988). Each FTE should generate a time-dependent flow signature in the ionosphere, two forms for which have been predicted. The first form is due to the motion of the point where the tube

*Also Visiting Honorary Lecturer, Imperial College, London SW7 2BZ, U.K.

of newly reconnected flux threads the magnetopause (due to magnetic tension and magnetosheath flow) which is transmitted to the ionosphere by a pair of oppositely directed filamentary field-aligned currents on the flanks of that tube (SOUTHWOOD, 1985, 1987; COWLEY, 1986). The second flow signature results from the twisted nature of the reconnected tube, as observed by SAUNDERS *et al.* (1984). WRIGHT (1987) has argued topologically that a maximum of a half twist arises from the initial shear in the magnetic field at the magnetopause and SOUTHWOOD *et al.* (1988) show that a twist will also result from the velocity shear. As the tube subsequently untwists, it generates a rotation of ionospheric plasma, within the region of newly reconnected flux, transmitted by a coaxial field-aligned current system, as predicted by LEE (1986). In general, the ionospheric signature is expected to be the superposition of these convecting and rotating flux tube patterns (MCHENRY and CLAUER, 1987; BERING *et al.*, 1988; LOCKWOOD *et al.*, 1990a).

The first suggestions of FTE signatures in the ionosphere were by VAN EYKEN *et al.* (1984) and GOERTZ *et al.* (1985). In their paper, van Eyken *et al.* described a burst of poleward flow in the dayside auroral oval, observed during one of the initial runs of the EISCAT 'Polar' experiment. This event lasted about 10 min and these authors suggested that it could have been caused by the motion of the ionospheric footprint of newly opened flux in an FTE. GOERTZ *et al.* (1985) described several bursts of poleward flow across the convection reversal boundary in spatial flow plots from the STARE radar. The conjugate GEOS spacecraft passed through the magnetopause into the magnetosheath, showing the open/closed field line boundary was indeed within, or at least close to, the STARE field-of-view (i.e. at unusually low invariant latitudes). The GEOS magnetometers were not capable of observing the standard characteristic signatures of FTEs; however, Goertz *et al.* argued that the lack of dispersion in the particle drop-outs seen by the spacecraft was inconsistent with a compressional motion of the magnetopause past the satellite (caused by enhanced solar wind and/or magnetosheath dynamic pressure). Hence, they inferred that a burst of reconnection, i.e. an FTE, took place a few minutes prior to each flow burst seen by STARE.

In their initial interpretation of magnetopause magnetometer data in terms of transient magnetic reconnection, RUSSELL and ELPHIC (1978) invoked a circular reconnected flux tube model. As a result, several authors have used circular or near-circular open flux tubes in the ionosphere to predict the ionospheric flow and current patterns for comparison with observations (LANZEROTTI *et al.*, 1986, 1987; TODD *et al.*,

1986; LOCKWOOD *et al.*, 1988a; BERING *et al.*, 1988; LOCKWOOD and SMITH, 1989). However, the multi-*X*-line theory of FTEs by LEE and FU (1985) and the time-varying reconnection rate theory by SOUTHWOOD *et al.* (1988) and SCHOLER (1988) predict that the flux tube (at all altitudes) may be considerably elongated in the East-West direction. Furthermore, CROOKER and SISCOE (1990) have shown that the ionospheric foot of the flux tube can be similarly elongated, even for a circular tube at the magnetopause: this mapping assumed the magnetosphere was closed other than for the FTE tube. In the more general case of an FTE appended to an open polar cap, CROOKER (1990) finds the FTE signature can indeed be nearly circular. LOCKWOOD *et al.* (1990a) have recently reported radar and optical signatures of flow bursts which were very like FTEs in their occurrence and which were indeed elongated in their East-West dimension. These authors, and also WEI and LEE (1990), predicted the flow patterns around such elongated tubes of elliptical cross-section.

The SOUTHWOOD (1985, 1987) model of the ionospheric signature of a flux transfer event predicts a twin vortical flow pattern. A further complication in the search for such effects has been the ability of dynamic pressure pulses in the solar wind to also produce twin vortical flows. Indeed, the vortical flow events and equivalent magnetometer signatures discussed by TODD *et al.* (1986) and LANZEROTTI *et al.* (1987) have been shown by SIBECK *et al.* (1989) to be associated with dynamic pressure changes in the upstream solar wind. FARRUGIA *et al.* (1989) have observed such ionospheric signatures in association with a major solar wind dynamic pressure increase and observed the resulting magnetospheric compression. These authors noted that although the IMF was strongly northward, an orientation for which FTEs are observed only very rarely, magnetometers near the dayside auroral oval observed impulsive signatures very similar to those predicted for a single station due to an FTE (MCHENRY and CLAUER, 1987). The induction of these vortical flows in the ionosphere by dynamic pressure changes has been explained by SOUTHWOOD and KIVELSON (1990) and LEE (1991) in terms of the effects of magnetic field and plasma density gradients in the low-latitude boundary layer. ELPHIC (1988) demonstrated the consistency of the predicted magnetopause motions caused by dynamic pressure changes with the large and rapidly moving twin vortical patterns observed by FRIIS-CHRISTENSEN *et al.* (1988) and GLASSMEIER *et al.* (1989). LOCKWOOD *et al.* (1990a) have discussed how such vortices can be distinguished from FTE effects.

The relative importance of quasi-steady reconnection and FTEs as mechanisms for exciting convection in the ionosphere and magnetosphere is not yet clear. In addition, the theoretical work of SOUTHWOOD and KIVELSON (1990) and LEE (1991) demonstrates that both increases and decreases in dynamic pressure must also be considered as such a convection-driving mechanism, as suggested originally by DESSLER (1964). Studies using passes of low-altitude polar orbiting spacecraft show the transpolar voltage is typically 100 kV for strongly southward IMF [see reviews by COWLEY (1984) and REIFF and LUHMANN (1986)]. Interpretation of magnetopause FTE signatures with the RUSSELL and ELPHIC (1978) circular flux tube model yields reconnection voltages (appearing along the X -line) of about 10 kV associated with each event. However, the elongated neutral line theories of LEE and FU (1985), SOUTHWOOD *et al.* (1988) and SCHOLER (1988) give voltages larger than this figure by a factor roughly equal to the length of the reconnection X -line (or lines in the Lee and Fu model) in Earth radii [$1R_E$ being the typical diameter of a Russell and Elphic flux tube (SAUNDERS *et al.*, 1984)]. For an X -line of length $10R_E$ these models would therefore predict reconnection voltages of order 100 kV. It should be noted, however, that from the duration of FTE signatures at the magnetopause, it is estimated that reconnection proceeds for typically 2 min whereas they recur only every 8 min on average (BERCHEM and RUSSELL, 1984; RIJNBEEK *et al.*, 1984). Hence, the mean contribution to the transpolar voltage by FTEs is likely to be about one-quarter of the FTE reconnection voltage, i.e. about 25 kV for the Southwood *et al.*/Scholer models. The voltage due to dynamic pressure changes should be limited to the 30 kV observed when the IMF is northward, unless some mechanism is present which makes the response of the magnetosphere to a pressure change depend upon the IMF B_z component.

If detected and correctly interpreted, observations of resulting ionospheric flows offer a unique opportunity to quantify the contributions of the mechanisms of transient momentum transfer to the total transpolar voltage. This is because a network of ionospheric observatories can define the spatial extents of events. Furthermore, studies of the ionospheric response time to changes of the IMF can tell us much about how convection is excited and determine whether or not the flows are in equilibrium with the IMF. Ground-based ionospheric flow observations are of particular importance in these areas because the field-of-view rotates with the Earth, and hence moves only a very small distance during the relevant time scales of order 1–10 min. *In-situ* data from low-

altitude polar-orbiting spacecraft, by contrast, suffer from spatial/temporal ambiguity problems as the satellite moves a considerable distance in such periods.

2. OBSERVATIONS

An ideal opportunity to study the response of ionospheric convection to changes in the IMF was presented by the AMPTE (Active Magnetospheric Particle Tracer Explorer) mission, in conjunction with ionospheric flow data from the EISCAT (European Incoherent Scatter) radar (WILLIS *et al.*, 1986). The AMPTE IMF data were recorded by the UKS (UK Satellite) and IRM (Ion Release Module) spacecraft immediately upstream from the Earth's subsolar bow shock and hence the satellite-to-magnetopause propagation delay could be computed with uniquely low errors. The largest sources of error are the estimated locations of the bow shock and magnetopause and the assumed ratio of the mean magnetosheath flow speed to that of the solar wind upstream from the bow shock. None the less, TODD *et al.* (1988b) estimate an uncertainty in the spacecraft-to-magnetopause delay of only ± 1 min. The EISCAT data were recorded using the 'Polar' experiment mode, which uses the beamswinging technique to derive flow vectors with relatively high time resolution over a range of invariant latitudes. Limitations to the AMPTE satellite tracking mean that simultaneous data could only be recorded while EISCAT was observing the dayside ionosphere.

The Polar experiment mode of the EISCAT radar has been described by VAN EYKEN *et al.* (1984) and WILLIS *et al.* (1986). The radar is operated monostatically with signals transmitted and received at Tromsø, Norway. The radar beam is swung at a low elevation (21.5°) between two azimuths 12° either side of the northward magnetic meridian (see Fig. 1). The beam dwells at each azimuth for 2 min and takes 30 s to travel between them, giving a total beamswinging cycle period of 5 min. Data are continuously pre-integrated and recorded, originally at 15-s intervals: in later (post-1987) versions of the experiment these intervals were reduced to 10 s. The data are divided into range gates 75 km apart in the SP-UK-POLA and CP-4 versions of the experiment, but this resolution was improved to 37.5 km in the SP-UK-POLI version. The latitude range accessed by the experiment depends upon the solar cycle: in 1984, SP-UK-POLA yielded good 15-s data over the range of invariant latitudes of roughly 71° – 73° , whereas by 1989 SP-UK-POLI made equivalent 10-s observations over 71° – 76° . For 2-min post-integrated data the greater signal-to-noise ratio

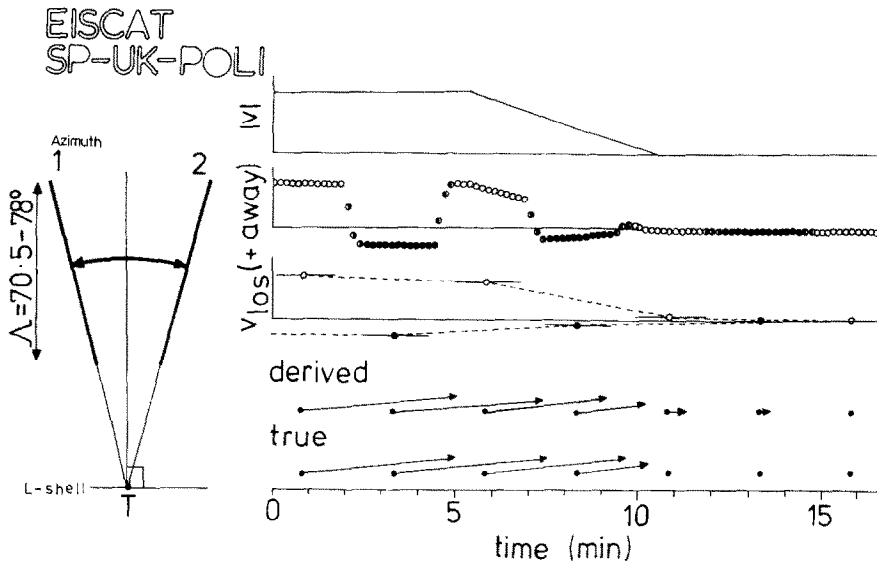


Fig. 1. The observation of plasma flows using the 'Polar' mode of the EISCAT radar. The viewing geometry of the two look directions (azimuths 1 and 2) are shown on the left: the range of invariant latitudes shown is that covered at sunspot maximum and T is the transmit/receive site at Tromsø. The top and bottom panels on the right-hand side show a model variation of the flow magnitude, $|v|$, and true flow vectors which are always slightly to the north of eastward in this example. The second panel shows the line-of-sight velocities, v_{los} , that would be observed by one range gate in each 10-s pre-integration period (positive away from Tromsø): solid circles are for azimuth 1, open circles are for azimuth 2, and half-solid circles are while the antenna is in motion. The flow is assumed to be uniform over the separation of the two scattering volumes for that range gate. The amplitude of the 'square-wave' modulation imposed by the beamswinging reflects the decrease in eastward flow. The third panel shows the v_{los} values, post-integrated over the 2-min antenna dwells. Adjacent values from one azimuth are averaged (i.e. linear interpolation) and compared with the observed value for the other azimuth. This yields the derived vectors shown. Comparison of the true and derived vectors (the two lower panels) shows the effects of smoothing and, to a lesser extent in this case, 'mixing', as discussed by ETEMADI *et al.* (1989).

increases these ranges to $71\text{--}74^\circ$ and $71\text{--}78^\circ$, respectively. The field-of-view is at an MLT approximately given by $\text{MLT} \approx \text{UT} + 2.75 \text{ h}$.

The flow data from the Polar experiment are interpreted in two ways. In the first, the line-of-sight data from the two azimuths are combined into vectors using the procedure described by WILLIS *et al.* (1986). This application of the beamswinging technique relies on a number of assumptions. These are principally that the flow is uniform over the radar field-of-view and that it varies linearly with time within the beamswinging cycle period. The effects of these assumptions have been studied by LOCKWOOD *et al.* (1988b) and ETEMADI *et al.* (1989), respectively. Figure 1 demonstrates how the vectors are derived. Consider the model 'true' flow vectors shown in the bottom panel, which show flow always directed slightly to the north of eastward but decreasing in flow magnitude, $|v|$, in a 5-min period, as shown in the top panel. The second panel shows the 10-s line-of-sight velocities

(V_{los}) which would be observed by the radar (if the received signal-to-noise ratio is high). The solid circles are observed while the antenna is at azimuth 1, open circles while it is at 2 and half-solid circles while it is in motion between 1 and 2. These v_{los} data are post-integrated into the 2-min dwells of the antenna, as shown in the third panel, and each value compared with the average value for the preceding and following dwell at the other azimuth. This comparison yields 'derived' vectors every 2.5 min, as shown in the figure. Comparison of the true and derived vectors shows both the effects noted by ETEMADI *et al.* (1989) of 'mixing', whereby spurious values in one component are induced by changes in the other, and smoothing. For this gradual (5 min) change in the real flow, the differences between the true and derived vectors are, however, much less marked than in the step-function case described by Etemadi *et al.*

A second way of viewing these flow data has been introduced by TODD *et al.* (1988a) and applied by

TODD *et al.* (1988b) and LOCKWOOD *et al.* (1988b). Panel 2 of Fig. 1 shows that the beamswinging introduces a 'square-wave' modulation into the sequence of v_{los} data when the flow is constant. The amplitude of this wave is proportional to the East–West flow and the mean value to the northward flow. The point-to-point consistency of the 10-s data points gives a check on the assumption that the flow is smoothly varying and the assumption of a linear variation with time can also be assessed.

3. THE RESPONSE OF DAYSIDE IONOSPHERIC FLOWS TO CHANGES IN THE B_z COMPONENT OF THE IMF

RISHBETH *et al.* (1985) and LOCKWOOD *et al.* (1986a) have discussed an example of a clear and sudden onset of strong ionospheric flow, as observed by EISCAT, just a few minutes after a swing of the IMF from northward to southward, as observed by the AMPTE-UKS satellite. This example is also discussed by LOCKWOOD and COWLEY (1988) and LOCKWOOD and FREEMAN (1989). This review aims to stress two facts: firstly, that both northward and southward turnings of the IMF have marked and almost immediate effects on the pattern of dayside high-latitude plasma convection; secondly, that such responses are common in the EISCAT-AMPTE dataset.

Figure 2 is an example of the combined IMF and ionospheric flow data observed by AMPTE-IRM and EISCAT, respectively. The top panel shows the IMF B_z (GSM coordinates) observed at the UT given by the top scale. The lower panels show the EISCAT data observed at the UT given by the bottom scale (MLT \approx 1455–1525, i.e. mid-afternoon sector). The two time scales have been offset by the predicted propagation delay from the satellite to the magnetopause [see LOCKWOOD and COWLEY (1988), FARRUGIA *et al.* (1989) and LOCKWOOD *et al.* (1989b)]. Hence the top panel can be regarded as an indication of the magnetosheath field orientation at the subsolar magnetopause and at the time of the EISCAT observations.

The IMF data show that B_z turned from negative to positive at 1213 UT. The middle panels show the line-of-sight velocities observed in gates 1–4, for which the received signal-to-noise ratio was sufficient to allow 15-s analysis of the data. These data show the square wave modulation discussed in the previous section, indicating flow just to the north of westward. The amplitude of this square wave begins to decrease at about 1220 UT. Allowing for the predicted propagation delay from IRM of approximately 5 min, this

is roughly 2 min after the northward turning reached the subsolar magnetopause. The decline in flow speeds was then observed over the subsequent 10 min. The smoothness of the data within the 2-min dwells shows that the beamswinging technique will not give rise to serious errors, although the linear interpolation assumption does not always strictly apply (because trends in line-of-sight velocity are not always seen to be continued in the next dwell at the same azimuth). The derived vectors are shown in the lower panels in Fig. 2. In this presentation vectors have been rotated through 90° to avoid congestion due to the largely westward flows: hence, northward flows are depicted by vectors pointing to the right and westward flows by vectors pointing to the top of the figure. These vectors show the general behaviour in the flows inferred above from the line-of-sight velocities, i.e. a decline in westward flow speeds over a period of roughly 10 min, but will contain some errors due to the beamswinging technique.

The northward turning of the IMF shown in Fig. 2 is one of the 10 clear northward turnings found by TODD *et al.* (1988b) in their survey of the 5 days of combined EISCAT-AMPTE observations. This survey also found 10 clear southward turnings. For each of these events, Todd *et al.* computed the 'ionospheric response time' between the IMF change impinging upon the subsolar magnetopause and the onset of the ionospheric flow response. The results showed that the short response time shown in Fig. 2 is typical, with both northward and southward turnings giving values of 2–5 min in the early afternoon sector, increasing to near 15 min near dawn and dusk. These results supported the findings of ETEMADI *et al.* (1988), who carried out a statistical cross-correlation analysis of all the EISCAT-AMPTE data using the components of the derived flow vectors. These results demonstrate the direct control of the dayside flow pattern by the IMF, the flows responding with delays of order 5 min. These delays are similar to those found statistically for the DP-2 current system by NISHIDA (1968a,b) and in various case studies of geomagnetic disturbance (PELLINEN *et al.*, 1982; NISHIDA and KAMIDE, 1983; MCPHERRON and MANKA, 1985; CLAUER and KAMIDE, 1985). SERGEEV *et al.* (1986) have found similar delays of increases and decreases of polar cap convection (inferred from polar cap magnetograms) following, respectively, 27 southward and 54 northward turnings of the IMF.

The EISCAT-AMPTE observations reported by TODD *et al.* (1988b) and ETEMADI *et al.* (1988) were all made while EISCAT was observing the dayside auroral oval. LOCKWOOD *et al.* (1990b) have presented an example of a rapid decline of the flow observed

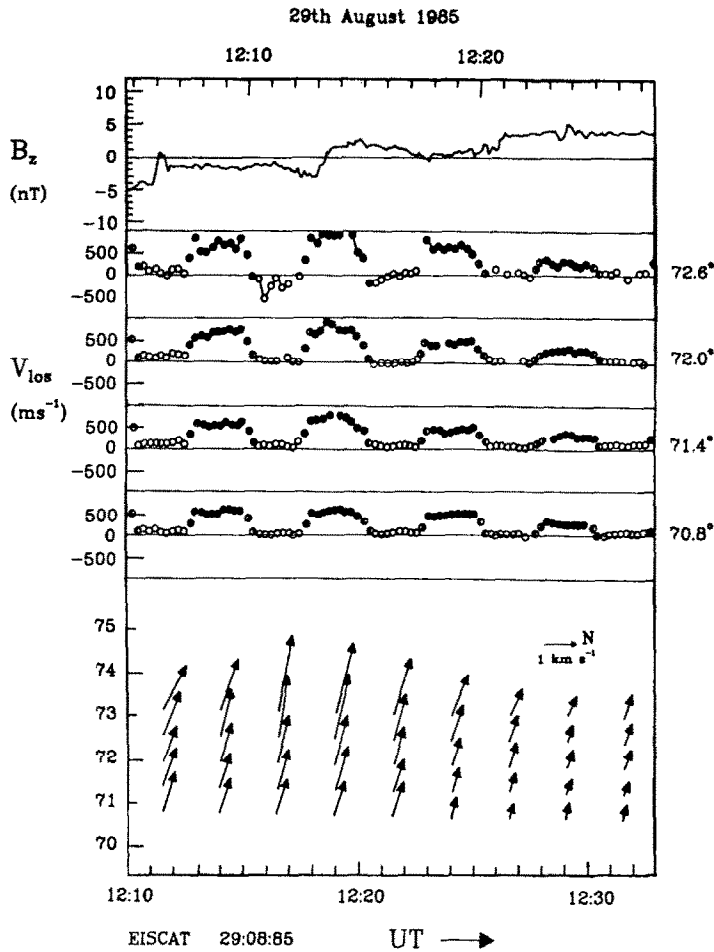


Fig. 2. EISCAT-AMPTE observations of a response in ionospheric flow to a change in the IMF. The top panel shows the northward component of the IMF (in GSM coordinates), observed by the AMPTE-IRM satellite on 29 August 1989 at the UT given by the top scale. The lower panels show the flow observations made simultaneously by EISCAT at the UT given by the bottom scale. The two UT scales have been offset by the predicted satellite-to-magnetopause propagation delay. The data show the line-of-sight velocities, v_{los} , and derived flow vectors for range gates 1-4 and 1-5, respectively, using the method and notation described in Fig. 1. Note that, in order to avoid congestion of the largely westward flow vectors, these have been rotated through 90° so vectors pointing to the right denote northward flow and those pointing to the top of the figure denote westward flow. A slowing of the flow is observed at 1220-1230 UT (when the EISCAT field-of-view is at about 1505-1515 MLT), shortly after the northward turning of the IMF seen by IRM at 1213 UT.

within the polar cap, as defined by both the convection reversal and by photometer observations of the poleward edge of the dayside aurora. The flows on this day are shown at the top of Fig. 3, using the same format as in Fig. 2. The dashed line is the position of the poleward edge of the 630 nm aurora, as observed by a photometer at Ny-Ålesund, Spitzbergen, scanning a meridian roughly 150 km to the east of that of the radar: the locations of the 630 nm aurora are

computed for an estimated emission altitude of 250 km. The middle part of Fig. 3 shows the voltage observed across gates 1-7 of the radar, $\varphi_{1,7}$, derived by integrating the observed northward component of the electric field (hence positive $\varphi_{1,7}$ denotes net westward flow in the radar field of view and negative values denote net eastward flow). Note that this procedure assumes that the ions are drifting with velocity, $\mathbf{v} = \mathbf{E} \times \mathbf{B} / B^2$. This is a valid assumption as Polar

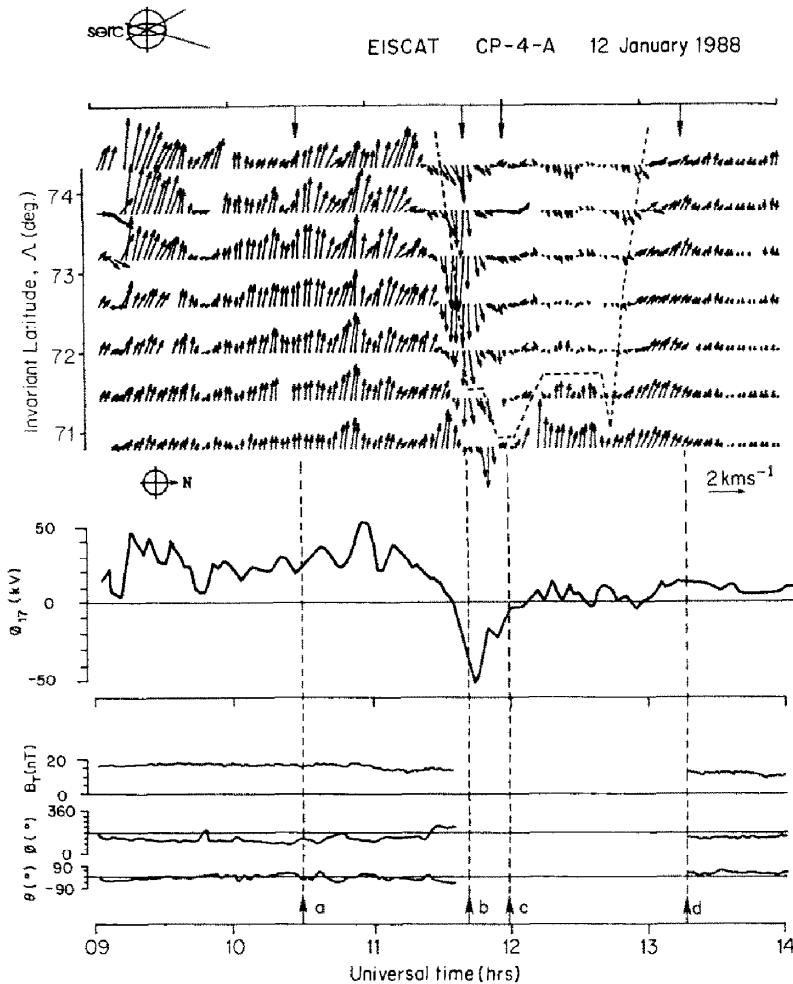


Fig. 3. Ionospheric plasma flow and IMF data for 12 January 1988. The top panel shows the flow vectors observed by EISCAT (with the 90° rotation employed in Fig. 2). The dashed lines show the poleward edge of the 630 nm aurora (where intensity falls below 1 kR), estimated from a meridian scanning photometer at Ny-Ålesund using an assumed emission altitude of 250 km. The middle panel shows the potential, ϕ_{17} , across the first seven radar gates, deduced by integrating the northward electric field component (corresponding to the westward component of the flows shown). The lower three panels show the strength, azimuthal angle (φ) and elevational angle (θ) of the IMF observed by IMP-8 and in GSE coordinates. The times marked a-d are referred to in the text and in Fig. 4.

makes observations in the F -region (at altitude 210 km for range gate 1 and increasing with gate number) where the effects of thermospheric winds on field-perpendicular ion motions can be neglected. The lowest three panels of Fig. 3 show the IMF strength and orientation observed by the IMP-8 spacecraft.

Initially (for example at 1030 UT—marked time *a*), the flow was westward. The flows observed were auroral for this afternoon sector (MLT \approx 1315 for time *a*). The voltage ϕ_{17} showed a series of peaks which

will be discussed later in this paper. After 1130 UT, a reversal to eastward flow then propagated from north to south across the radar field-of-view, followed by a similar motion of the poleward auroral boundary. As a result, by time *b* (1145 UT) strong eastward flow ($2\text{--}3\text{ km s}^{-1}$) was observed in gates 3–7. However, this flow subsequently decayed to weak northward flow (200 m s^{-1}) within about 5 min, such that by time *c* (1200 UT) virtually no flow was observed by the radar. This rapid decay of the flow occurs poleward

of the poleward edge of the dayside aurora and poleward of the afternoon sector convection reversal boundary from westward to eastward flow. The voltage φ_{17} changed from -55 kV to near zero between b and c . It should be noted that a potential difference as large as 55 kV strongly indicates that most of this eastward flow was driven by reconnection and hence supports the inference that the further range gates were within the open field line region (as deduced from the southerly location of the aurora). Unfortunately, the flow decay occurs within a gap in the IMP-8 data during which both B_z and B_y changed sense. Lockwood *et al.* argue from the simultaneous flow data recorded by the Sondrestrom radar that the initial slowing at EISCAT was due to a change in the B_y component of the IMF and that the subsequent contraction of the polar cap and convection boundaries near 1300 UT were due to the northward turning of the IMF. However, the cause of the slowing is not as important as the fact that it occurred within the polar cap and on the short time scales observed by TODD *et al.* (1988b). The decay times of 5–10 min mean that open field lines have ceased moving whilst remaining largely within the radar field-of-view. For a flow change this rapid, we can consult the 10-s data to ensure the vector data are not in error, due to the beamswinging technique. The 10-s line-of-sight velocities are shown in Fig. 4 and show point-to-point consistency but there was variation within each antenna dwell. Interpreting these data in terms of the model eastward flow decay shown in Fig. 1 indicates that the slowing was more rapid than indicated by the smoothed vectors, occurring mainly at 1145–1150 UT for gates 3–6, well inside the polar cap. Figure 4 also shows that after the slowing the character of the flow is quite different, with weak, smooth northward flow seen in all gates (e.g. time c).

4. THE EFFECT OF OPEN FIELD LINES

The observations presented in the previous section have important implications for how convection is excited. Firstly, there is the fact that dayside auroral zone flows slow rapidly (within 2–15 min) after the IMF has turned northward. Secondly, open field lines within the polar cap can virtually cease moving on similar short time scales. It is highly unlikely that for all the events discussed by TODD *et al.* (1988b), the EISCAT radar was, by chance, in the correct location to observe a local effect. We must therefore conclude that TODD *et al.* (1988b) were indeed observing a global response. That these rapid (minute) variations in convection electric fields can indeed be global is

confirmed by high-time resolution studies using magnetometer and radar networks (REIFF *et al.*, 1985; RICHMOND *et al.*, 1988). LOCKWOOD *et al.* (1990b) have pointed out that these facts do not allow all open field lines to be equally effective in exciting ionospheric flow. Were all open field lines equally effective, then convection could only decay on the time scales for contraction and expansion of the polar cap. Those time scales are known to be large from both observations (e.g. HOLZER *et al.*, 1986) and from the fact that the polar cap is such a large reservoir of magnetic flux (compared with the flux transfer rates into and out of the polar cap). That this is the case is demonstrated by Faraday's law, applied to the polar cap (CORONITI and KENNEL, 1973):

$$d\left(\int_A \mathbf{B}_i \cdot d\mathbf{A}\right)/dt = \varphi_d - \varphi_n \quad (1)$$

where B_i is the ionospheric magnetic field, A is the polar cap area, φ_d is the voltage associated with reconnection at the dayside magnetopause (i.e. with the opening of field lines) and φ_n is the voltage associated with the closing of field lines in the geomagnetic tail. In steady state $\varphi_d = \varphi_n$, and A is constant. Taking B_i to be constant at $5 \cdot 10^{-5}$ T and a circular polar cap of radius 2000 km, we find a typical value of the total flux into the polar cap of $B_i A$ of $6 \cdot 10^8$ Wb. This must be compared with peak φ_d and φ_n values of order 100 kV (i.e. 10^5 Wb s $^{-1}$) and gives time constants for significant polar cap expansion and contraction of several hours, as observed (HOLZER *et al.*, 1986). Hence, the global response of convection to changes in the IMF on short time scales indicates that not all open field lines are responsible for exciting convection.

The observations by LOCKWOOD *et al.* (1990b) that the ionospheric feet of open field lines can cease moving on short time scales is important because those open field lines remain connected to the IMF at the magnetopause and the point where they thread the magnetopause moves continuously anti-sunward with the magnetosheath flow. As a result, these authors conclude that the interplanetary electric field does not in general map down all open field lines into the polar cap, as has often been assumed (STERN, 1973; LYONS, 1985; RYCROFT, 1987; TOFFOLETTO and HILL, 1989). That the electric field does not map down open field lines does not necessarily imply the presence of field-aligned voltages. More simply, there is a curl in the electric field, and hence the magnetic field in the lobe is changing with time as field lines are stretched down the tail.

LOCKWOOD and FREEMAN (1989) have pointed out that the expanding–contracting polar cap model of

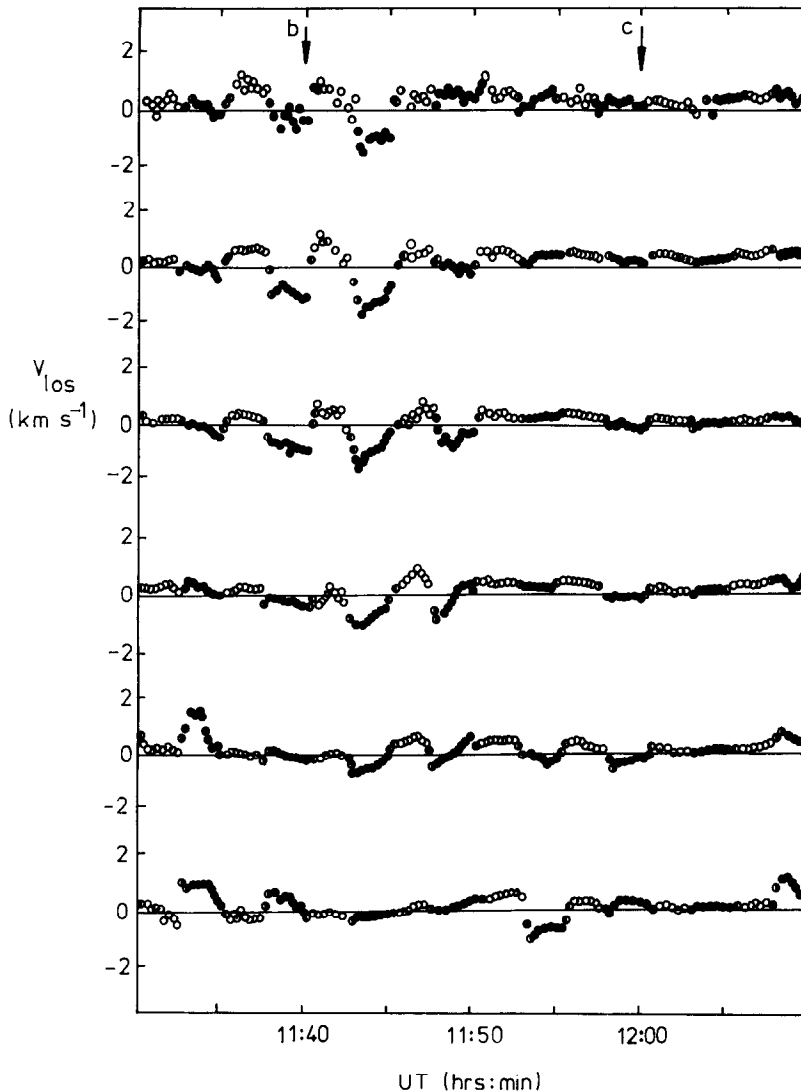


Fig. 4. Line-of-sight velocities observed by EISCAT on 12 January 1988. The data are shown using the symbols introduced in Fig. 1. The times b and c are also marked in Fig. 3.

ionospheric convection proposed by SISCOE and HUANG (1985) [see also RUSSELL (1972)] offers a unified description of these effects. This model is demonstrated by Fig. 5 (from LOCKWOOD *et al.*, 1990b). Part (a) shows the equipotentials (flow streamlines) modelled by Siscoe and Huang for wholly unbalanced reconnection at the dayside magnetopause ($\varphi_d = 0$), whereas (b) shows the equivalent flows for unbalanced reconnection in the geomagnetic tail ($\varphi_d = 0$). Parts (c) and (d) give more general cases where reconnection is present at both the dayside magnetopause

and in the geomagnetic tail but with $\varphi_d > \varphi_n$ (expanding polar cap) and $\varphi_d < \varphi_n$ (contracting polar cap), respectively. It can be seen that convection at all locations within the polar cap and auroral oval is influenced by both dayside and nightside reconnection. However, flows on the dayside are dominated by dayside reconnection and nightside flows by reconnection in the tail. Implicit in this view of convection is the concept that flow is excited only when reconnection has recently been in progress. Hence dayside flows will respond rapidly to changes in the IMF [as

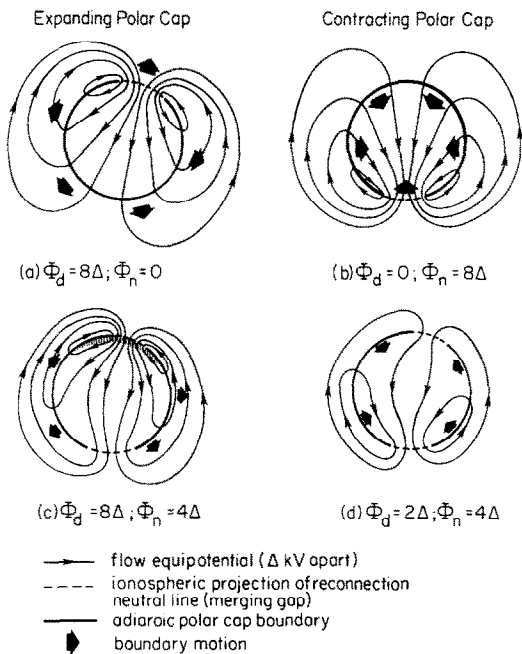


Fig. 5. Schematic examples of ionospheric convection patterns for expanding (left) and contracting (right) polar caps from the model by SISCOE and HUANG (1985). The voltage φ_d is that across the dayside merging gap due to reconnection at the dayside magnetopause, φ_n is that across the nightside gap due to reconnection in the geomagnetic tail: equipotentials are shown Δ kV apart. Solid lines show 'adiaroic' boundaries where no flux enters or leaves the polar cap. (a) $\varphi_d = 8\Delta$, $\varphi_n = 0$; (b) $\varphi_d = 0$, $\varphi_n = 8\Delta$; (c) $\varphi_d = 8\Delta$, $\varphi_n = 4\Delta$; and (d) $\varphi_d = 2\Delta$, $\varphi_n = 4\Delta$. A northward turning of the IMF would give a rapid (within a few minutes) change from a pattern like (c) to one like (d), with a sudden decrease in the dayside flow in both the polar cap and the auroral oval.

observed by TODD *et al.* (1988b) and ETEMADI *et al.* (1988b)] and nightside flows will respond rapidly to changes in reconnection rate in the tail (as observed during substorms).

The Siscoe and Huang model also offers an explanation of another feature of the EISCAT-AMPTE data. LOCKWOOD *et al.* (1986a) noted that following the southward turning of the IMF presented by RISHBETH *et al.* (1985), the ion temperature enhancement (and hence the enhanced flows) propagated eastward around the afternoon sector and over the radar field-of-view after a short (1–2 min) lag. Lockwood *et al.* showed that the lag and expansion speed were consistent with newly opened flux being appended to the polar cap following the onset of dayside reconnection due to the southward turning. The surprising result, however, was that the flows associated with the region of newly opened flux were so much greater than those

prior to the southward turning, driven by the adjacent, 'old' polar cap. This is consistent with Fig. 5, and demonstrates that the presence of newly opened field lines is vital for the excitation of dayside convection, not the presence of any open flux. In other words, it is the transfer of flux from the dayside into the tail lobe which excites convection, not the existence of open field lines. Consider the evolution of open field lines following a northward turning: the convection at their ionospheric feet will be slow [at least on the dayside as shown in parts (b) and (d) of Fig. 5] while their antisolar motion at the magnetopause proceeds unabated. In general, therefore, the interplanetary electric field does not map down open field lines.

LOCKWOOD *et al.* (1986) explained the eastward expansion they observed in terms of the growth of the region of newly opened flux as reconnection proceeds following its onset at the southward turning. The expansion speed derived (2 km s^{-1}) is quantitatively consistent with the increase in response delay with distance from noon, as observed by TODD *et al.* (1988b) and ETEMADI *et al.* (1988) [see discussion by LOCKWOOD *et al.* (1990b)].

It should be noted that, in the foregoing discussion, various complicating factors have been omitted. These include the differences between the voltages along the reconnection neutral lines and the corresponding voltage along their ionospheric projections (the merging gaps), due to their motion. In addition, a viscous-like interaction can be allowed for by generalizing the potential distribution along the polar cap boundary (e.g. COWLEY, 1982) and reconnection at the tail lobes during northward IMF yields either additional circulation in one polar cap (reconnection taking place at only one lobe) or a negative value φ_d (reconnection at both lobes) (RUSSELL, 1972). These factors are all considered in greater detail by LOCKWOOD *et al.* (1990b). LOCKWOOD *et al.* (1988b) have observed the viscous-like electric field along the ionospheric polar cap boundary away from the merging gaps. The total voltage due to this electric field is estimated to be less than 20 kV, consistent with satellite observations of the residual cross-cap potential difference during periods of northward IMF and with the voltage observed across the magnetopause boundary layer [see review by COWLEY (1984) and LOCKWOOD *et al.* (1988b)]. Such potentials are small compared with the values observed during southward IMF and associated with reconnection: peak values of 130 kV have been derived from satellite passes (COWLEY, 1984; REIFF and LUHMANN, 1986) and LOCKWOOD *et al.* (1986b) have observed a polar cap expansion showing that φ_d briefly exceeds φ_n by as much as 200 kV [by

equation (1)]. Hence viscous-like momentum transfer will not significantly alter Fig. 5, particularly during periods of strongly southward IMF and/or strong magnetic activity.

Evidence for the bimodal nature of high-latitude convection, as shown in Fig. 5, has, in fact, been available from magnetometer observations of ionospheric currents. Geomagnetic disturbances at high latitudes have been divided into two main morphological types, termed DP-1 and DP-2. The DP-2 system has been found to respond to changes in the IMF on very short time scales (typically after a few minutes) (NISHIDA, 1968a,b; SERGEEV *et al.*, 1986; PELLINEN *et al.*, 1982; NISHIDA and KAMIDE, 1983; MCPHERRON and MANKA, 1985; CLAUER and KAMIDE, 1985). On the other hand, analysis of indices like AE, which are primarily influenced by the nightside currents and in particular the DP-1 system, have indicated much longer response delays of 30–60 min (SCHATTEN and WILCOX, 1967; ARNOLDY, 1971; BAKER *et al.*, 1981, 1983). Two distinct response time scales were also revealed by studies of geomagnetic activity using the linear prediction filter technique (CLAUER *et al.*, 1981; BARGATZE *et al.*, 1985). KAMIDE *et al.* (1986) and KAMIDE and VICKREY (1983) conclude that the electric field plays the dominant role in ionospheric current variability, rather than the conductivity. Hence, in the same way that it is necessary to divide the high-latitude current system into the DP-1 and DP-2 systems, so the convection pattern must be a superposition of two parts, as in Fig. 5.

LOCKWOOD *et al.* (1990b) conclude that ionospheric convection must be thought of as the superposition of two flow patterns. The first is driven mainly by reconnection at the dayside magnetopause and is associated with the voltage ϕ_d . By equation (1) this pattern is therefore associated with an expanding polar cap area and, as demonstrated by Fig. 5, will dominate flows in the dayside high-latitude ionosphere. This flow pattern is equivalent to the DP-2 'growth phase' current system. The second pattern is mainly driven by reconnection in the tail and is associated with the voltage ϕ_n . This pattern will be associated with a contracting polar cap area, will dominate flows in the nightside ionosphere and is the flow equivalent of the DP-1 'expansion phase' current system. Consequently, the ionospheric convection pattern is inadequately described in terms of the prevailing IMF alone, although this is less true on the dayside than on the nightside. We note that a further consequence of this view of convection is that the interplanetary electric field does not generally map down open field lines.

5. TRANSIENT FLOW BURSTS IN THE DAYSIDE AURORAL OVAL

TODD *et al.* (1986) reported a major burst in poleward flow (peak speed about 1 km s^{-1}) in the dayside sub-auroral ionosphere, observed using the Polar experiment. This burst lasted less than 1 min and these authors showed the line-of-sight velocities to be consistent with the SOUTHWOOD (1985, 1987) twin vortical FTE signature. However, doubt has recently been cast upon this interpretation because SIBECK *et al.* (1989) have shown the event was associated with a pulse in dynamic pressure in the solar wind. In this section, we wish to discuss some more recent Polar observations of flow bursts in the dayside auroral oval. These observations are significantly different from those reported by Todd *et al.* Firstly, they are near the poleward edge of the auroral oval, not sub-auroral. Secondly, they last for 5–15 min and hence can be studied by the beamswinging technique (although care must be taken because there will be errors introduced by the rapidly varying nature of the flow). Lastly, in the examples observed to date the largest flows ($3\text{--}4 \text{ km s}^{-1}$) are either eastward or westward.

Figure 6 presents an example of such a flow burst. Note that these flow data, unlike Fig. 2, are shown in a conventional format, with northward flow vectors pointing to the top of the figure. At the start of the period shown (0630 UT, equivalent to an MLT of about 0930), the data show a convection boundary reversal near $\Lambda = 76^\circ$. This reversal had been observed to move poleward through the field-of-view during the previous 2 h. The event of interest here commences at 0650 UT with a swing to southward flow equatorward of the convection boundary, followed by a very strong (6 km s^{-1}) burst of eastward flow, lasting until about 0705 UT. During the peak flow at 0700 UT, weak westward flow is seen immediately to the north and the south of the main flow burst. For such rapid changes in flow speeds, the beamswinging technique will undoubtedly introduce some errors. It is therefore instructive to look at the scalar quantities observed by the radar. Figure 7 shows the ion temperatures [parts (a) and (b)] and plasma densities [parts (c) and (d)] observed in gates 10 (on equatorward edge of burst) and gate 12 (close to its centre). Data from azimuth 1 are given as solid circles, those from azimuth 2 as open circles. The dashed lines show the ion temperature, T_i , predicted from the vector ion flow speed v , using the ion frictional heating equation:

$$T_i = T_n + m_n v^2 / 3k \quad (2)$$

where T_n and m_n is the neutral density and mass and

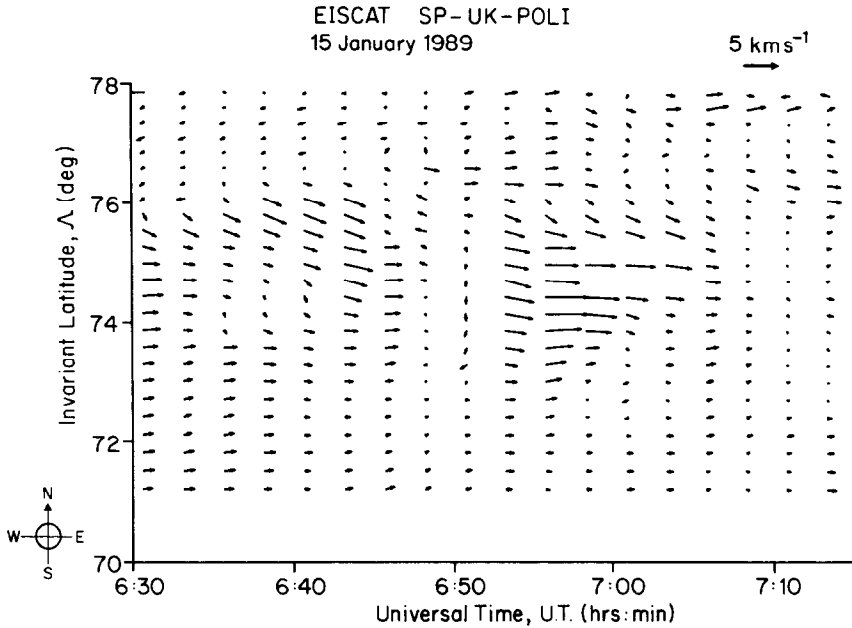


Fig. 6. Flows observed by EISCAT on 15 January 1989. Vectors are shown in convectional format with northwards pointing to the top of the figure. A strong burst of eastward flow is seen around invariant latitude, Λ , of 74.5 and UT of 0700 (MLT \approx 1000).

k is Boltzmann's constant. Equation (2) is valid when v is very large compared with the thermospheric wind speed (ST-MAURICE and HANSON, 1982), as is indicated by the vector data. The dashed lines in parts (a) and

(b) of Fig. 7 show the ion temperature derived using equation (2) with the value of v from the vector data. It can be seen that the observed temperatures peak near 20,000 K, as predicted from equation (2), but

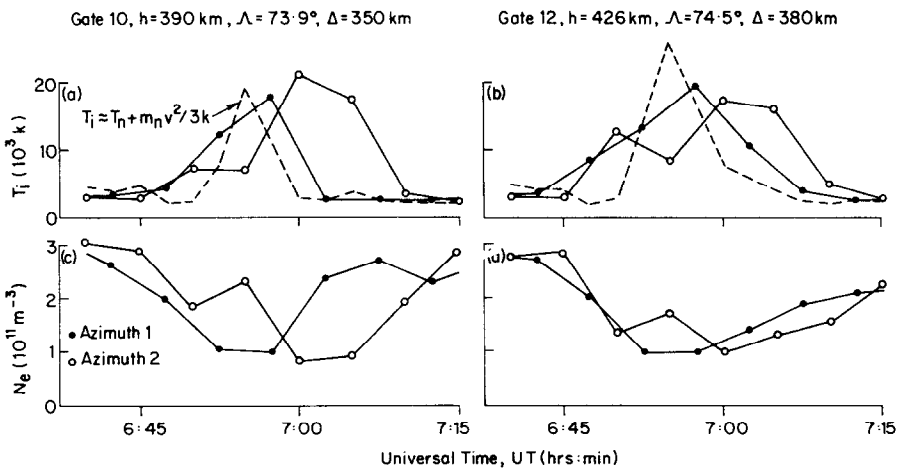


Fig. 7. Scalar plasma parameters observed during the event shown in Fig. 6. Solid circles are for azimuth 1, open circles are for azimuth 2. Plots to the left [(a) and (c)] are for gate 10, those to the right [(b) and (d)] are for gate 12: h is altitude, Λ the invariant latitude and Δ the separation of the azimuths at that range gate. The observed ion temperatures, T_i (from non-Maxwellian analysis), are shown in (a) and (b), along with the dashed line showing the value derived by equation (2) with the velocity, v , derived from the beamswinging technique. Parts (c) and (d) show the observed plasma density, N_e .

roughly 5 min after the peak in the dashed curves. We conclude that the peak flow speed of 6 km s^{-1} is substantially correct, but that the timing of the burst has been shifted by the beamswinging, as predicted by ETEMADI *et al.* (1989) depending upon the phase of the flow onset relative to the beamswinging cycle. The rises in T_i were accompanied by decreases in N_e , which is consistent with depletion of plasma by the enhanced rates of chemical reactions leading to plasma loss (SCHUNK and RAITT, 1980; EVANS *et al.*, 1983). A clear feature of Fig. 7 is that the two azimuths saw similar variations in both T_i and N_e , but that seen by azimuth 1 preceded that observed by azimuth 2, i.e. the effects were seen first in the western azimuth, implying an eastward motion of the flow feature over the radar field-of-view. The lag between the two azimuths is less than about 2.5 min for gate 12 and 2.5–5.0 min for gate 10. The East–West separation of the two scattering volumes is $\Delta = 380 \text{ km}$ for gate 12 and 350 km for gate 10. Hence the apparent speed of eastward motion is in excess of 2.5 km s^{-1} at gate 12 and $1.2\text{--}2.4 \text{ km s}^{-1}$ at gate 10. Given that the ion temperatures observed at the event centre, as shown in Fig. 7b, are not as large as predicted by equation (2) and hence that the derived flows may be somewhat overestimated, the event appears to have moved eastward with roughly the same speed as the eastward plasma flow speed within the event. As discussed by LOCKWOOD *et al.* (1990a), this is an important distinguishing feature of a convecting FTE signature in the ionosphere.

The dimensions of the event can also be estimated. The middle panel of Fig. 8 shows α , the North–South extent of the regions where flow speeds v exceed 1.0 km s^{-1} (dot-dash line) and 2.5 km s^{-1} (solid line). It can be seen that the outer region had a peak of about 500 km in North–South extent, whereas the inner region was just over 200 km wide. The top panel shows the potential across these regions, obtained by integrating the eastward flow speed, v_e (equivalent to southward electric field), over the dimension α . It can be seen that there is 55 kV across the inner region and 75 kV across the outer region. The East–West extent, β , can be estimated if it is assumed that a region of high-speed flow convects over the radar without changing shape or size, by integrating the observed eastward velocity with time. It should be noted that this assumes that every point within the region moves with the velocity of the region as a whole, as in the SOUTHWOOD (1985, 1987) FTE model. The results are shown in the bottom panel of Fig. 8, as a function of latitude. It can be seen that the regions are then found to be much larger in East–West extent (roughly 3000 km). This figure may be a slight overestimate (given

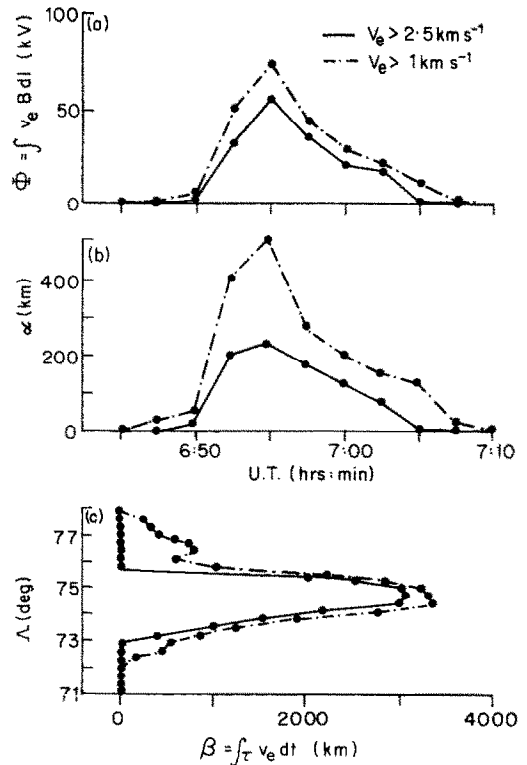


Fig. 8. Dimensions of the event described by Figs 6 and 7. The top panel shows the potential ϕ across the North–South dimension of the event, the length of which, α , is shown in the second panel. An estimate of the East–West dimension, β , derived using the assumption that a region of fixed size and shape convects through the radar field-of-view, is given in the lowest panel. The solid lines are for the region where the eastward flow speed, v_e , derived from the beamswinging technique, exceeds 2.5 km s^{-1} , the dot-dashed line is for where it exceeds 1.0 km s^{-1} .

that the ion temperatures indicate that the ion flows are somewhat overestimated). Nevertheless, an event of this length and of velocity exceeding 2.5 km s^{-1} would give an ion temperature enhancement (and plasma depletion) lasting something less than 20 min, consistent with Fig. 7.

It is not clear yet as to what mechanism drives the flows described in Figs 6–8. The peak flows are observed at an MLT of 1000. For such an MLT we would not normally expect nightside substorm processes to drive such strong flows. Sondrestrom data from MLT ≈ 0400 show a swing to weak eastward flow at this time (C. R. CLAUER, private communication, 1989), but very much smaller than the magnitude of the flows in Fig. 7. LOCKWOOD *et al.* (1988b), CLAUER *et al.* (1989) and ROBINSON *et al.* (1989) have recently discussed flow enhancements seen near

0400 UT by both EISCAT and Sondrestrom during a substorm and none of the characteristics of the flows shown in Fig. 7 is apparent. If the flows are not driven by a substorm, they are most likely to reflect some form of transient momentum transfer across the magnetopause. Data on the IMF are available for after 0652 from the IMP-8 satellite (R. P. LEPPING, private communication, 1989). At, and subsequent to, this time the IMF (in GSM coordinates) was consistently southward ($B_z \approx -3$ nT) and had a strongly negative Y -component ($B_y \approx -8$ nT). Hence the IMF orientation is consistent with a magnetopause reconnection interpretation of this event and the eastward (sunward) motion is as predicted for the magnetic tension effect on newly opened field lines.

Figures 6–8 demonstrate that considerable voltages can exist across small regions of the dayside auroral ionosphere. At the centre of this event we have 55 kV (a sizeable fraction of a typical transpolar voltage) across just 200 km. These voltages are transient, however, lasting 15 min in this case.

6. TRANSIENT DAYSIDE AURORAE ASSOCIATED WITH FLOW BURSTS

The islands of Svalbard, the largest of which is Spitsbergen, are unique in the northern hemisphere in that optical observations of the noon aurorae can be made from there around winter solstice (SAUNDERS, 1989b). Recent studies using meridian-scanning photometers and all-sky TV cameras have revealed transient auroral events throughout the dayside, in both the cusp and cleft regions (SANDHOLT *et al.*, 1985, 1989a,b, 1990; OGUTI *et al.*, 1988; SANDHOLT, 1988). One common type of transient has been termed 'mid-day auroral break-up'. Such events vary in their duration between 2 and about 15 min and tend to recur every 8 min. They are usually first observed as an intensification of the 630 nm 'red-line' aurora on the equatorward edge of persistent, background emissions. This intensification then drifts through and poleward of the background, frequently accompanied by an intense and structured transient 557.7 nm ('green-line') aurora. All-sky TV cameras (mainly sensitive to the 557.7 nm luminosity) see the intensification moving east or west into the meridian scanned by the photometers before drifting into the polar cap and fading. SANDHOLT *et al.* (1989b) have observed the energetic particles responsible for a simultaneously observed 557.7 nm transient, using the HILAT satellite in conjunction with the ground-based optical instrumentation. These particles were also found to be associated with structured, and probably fila-

mentary, field-aligned currents. Only a limited number of events have been observed for which there were simultaneous solar wind and IMF data; however, there are indications that events move west under positive IMF B_y conditions and east when B_y is negative (northern hemisphere). Furthermore, there is evidence that these events are only present when IMF B_z is negative. If confirmed by studies of much larger datasets, this means the zonal motions are consistent with the magnetic tension on newly opened flux tubes (COWLEY, 1981) and that the occurrence is very similar to that of flux transfer events at the magnetopause (BERCHEM and RUSSELL, 1984; RIJNBEEK *et al.*, 1984). Furthermore, LOCKWOOD *et al.* (1989a) have pointed out that the zonal-then-poleward pattern of motion is exactly as predicted for newly opened flux tubes (LOCKWOOD and FREEMAN, 1989), and as used by SAUNDERS (1989a) in his explanation of the cusp field-aligned currents. In effect, the ionospheric feet of newly opened flux tubes are subject to the magnetic tension forces as soon as they are connected to the IMF, and hence they move zonally under non-zero B_y conditions. Only a few minutes later, when the kink in the newly opened flux tube has straightened, will anti-solar magnetosheath flow produce poleward motion of the ionospheric part of the tube.

The suggestion that these events are ionospheric signatures of flux transfer events requires that they be accompanied by an ionospheric flow signature. Evidence that this is indeed the case is provided by part (0900–1130 UT) of the EISCAT data shown in Fig. 3. Figure 9 examines the period 1040–1105 UT [from LOCKWOOD *et al.* (1989a)]. Panel (a) shows the intensity of 630 nm emissions observed in 18-s scans by the photometer at Ny-Ålesund, Spitsbergen. Positive zenith angles are to the north of Ny-Ålesund. Panel (b) shows the corresponding scans by the 557.7 nm photometer. A transient optical event commenced near 1049 UT, with an intensification of the 630 nm aurora. At about 1054 UT, this event began to move poleward, accompanied by a burst of strong 557.7 nm aurora which also moved poleward. Both lines faded at about 1102 UT, some 13 min after the onset. This relatively long-lived event could be studied using the EISCAT 'Polar' experiment, with its 5-min beam-swinging cycle: some events last for just 2 min and hence could not be studied using this radar mode. Estimated emission altitudes of 130 and 250 km for the green and red lines, respectively, place the 557 nm luminosity close to the northern boundary of the radar field-of-view which is only 150 km to the west of the meridian scanned by the photometers. The peak 630 nm emission is found to be roughly co-located with the peak flow seen by the radar. Parts (c)–(e) of Fig.

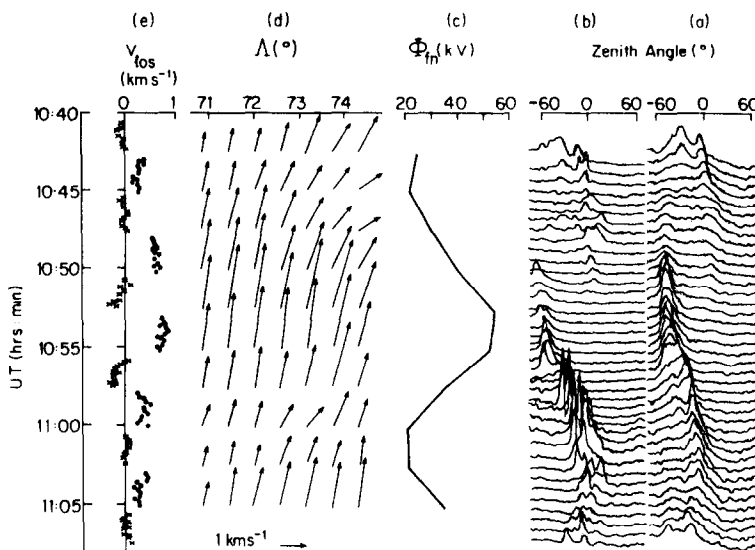


Fig. 9. Example of a dayside transient event observed by EISCAT and meridian scanning photometers at Ny-Ålesund, Spitsbergen, on 12 January 1988. Panels (a) and (b) show 18-s meridian scans by 630 nm and 557.7 nm photometers, respectively: positive zenith angles are to the north of Ny-Ålesund. Panel (c) shows the potential across the first seven gates of the EISCAT radar, ϕ_{17} , derived from the vectors shown in part (d) (in conventional format with northwards pointing to the top of the figure). Panel (e) shows the line-of-sight velocities, v_{los} , observed in gate 1.

9 show the radar data. The line-of-sight velocities observed in gate 1 are shown in part (e): they reveal a relatively smooth increase in 'square wave amplitude', peaking near 1052, followed by a smooth decrease. Accordingly, we would interpret these data as showing an increase and subsequent decrease in westward flow, as shown by the derived vectors [panel (d)]. Panel (c) shows the potential difference, ϕ_{17} , across the radar field-of-view. This voltage peaks at 55 kV: notice that the smoothing effect of the beamswinging technique will have tended to overestimate the duration of the flow burst but underestimate the peak voltage. Figure 9 shows that the transient aurora and the flow burst were largely concurrent, with the aurora lagging slightly after the peak voltage. Figure 10 demonstrates that this feature is a general one for the period 0900–1130 UT, shown in Fig. 3. The top panel (a) of Fig. 10 shows the voltage ϕ_{17} as a function of time, whereas (b) shows the zenith angle of the peak intensity in each scan of the 630 nm photometer. Only peak intensities exceeding 3 kR are shown in order to separate the transient events from the lower intensity, persistent background cleft/cusp aurora. The dashed arrows show that in nearly every case the peak in ϕ_{17} is very close to the onset of a 630 nm transient. LOCKWOOD *et al.* (1989b) have discussed the small peak in ϕ_{17} between events 4 and 5 and concluded it was

a separate event which had not been resolved from event 4 in the optical data. The small peak between events 5 and 6 does not appear to be associated with any optical signature. The event shown in Fig. 9 is that labelled '8' in Fig. 10. SANDHOLT *et al.* (1990) have studied in detail events 1 and 2, for which 1-s all-sky TV camera images were also available. They showed that the transient aurorae moved initially westward, before moving poleward, as described earlier. Furthermore, the velocity of the patch of auroral luminosity was always the same, to within measurement uncertainties, as the plasma drift seen in the nearest radar gates (see also LOCKWOOD *et al.*, 1990a).

The initial westward motion of all the events shown in Fig. 10 (positive ϕ_{17}) is consistent with the positive IMF B_1 component observed by the IMP-8 satellite (the azimuthal angle of the IMF, ϕ , is less than 180° in Fig. 3 at the relevant times and corresponds to a B_1 component of about 10 nT in GSM coordinates). The IMF also varied between southward and northward during this period (see the elevational angle θ in Fig. 3). LOCKWOOD *et al.* (1989b) have considered the IMF B_z component in GSM coordinates, allowing for the predicted satellite-to-magnetopause propagation delay. They conclude that between 0900 and 0945 UT, the sheath field at the subsolar magnetopause was

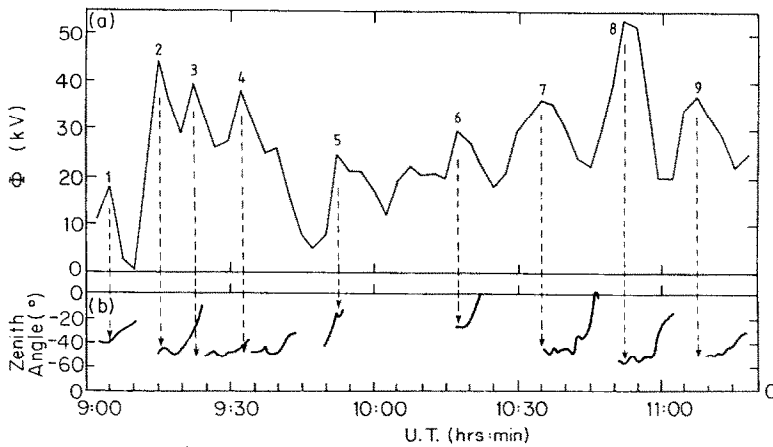


Fig. 10. Potential across the EISCAT radar, ϕ_{17} , and zenith angle of peak 630 nm emissions observed on 12 January 1988. The event labelled 8 is that shown in detail by Fig. 9. Only peak photometer intensities exceeding 3 kR arc shown to distinguish transient auroral intensifications from the persistent background dayside aurora. The dashed arrows show that the onset of each transient event is accompanied by a peak in the potential across the radar. The transient arcs are estimated (for an emission altitude of 250 km) to have been close to the peak flow observed by the radar.

almost continuously southward and that during this period the transient flow bursts, accompanied by transient auroral events and impulsive spikes on local magnetometers, were observed with a recurrence period of 8.3 ± 0.6 min. After 0945, the events were less frequent and could always be associated with a prior swing to southward IMF from the predominantly northward orientation. Furthermore, the peak voltage observed by the radar was correlated with the size of that southward swing. The recurrence period during the interval of continuously southward IMF is very similar to that found for magnetopause FTEs by BERCHEM and RUSSELL (1984) and RIJNBEEK *et al.* (1984). Solar wind data were not available for this period but LOCKWOOD *et al.* (1990a) have used decreases in IMF magnitude to infer the presence of significant dynamic pressure pulses. However, there is no correspondence of the occurrence of these with that of the transient auroral/flow burst events.

7. IMPLICATIONS OF DAYSIDE TRANSIENT EVENTS

Several theories have been put forward which may explain the transient events in the dayside auroral oval, as described in the previous section. As well as with FTEs (as discussed in the Introduction), these could be associated with 'impulsive penetration' of plasma into the magnetosphere (LEMAIRE and ROTH, 1978; LEMAIRES 1985; HEIKKILA, 1982; LUNDIN, 1988; HEIKKILA *et al.*, 1989) and/or dynamic pressure changes in the solar wind (SIBECK *et al.*, 1989; LEE, 1991).

It is not the purpose of the present paper to discuss the validity of these magnetopause mechanisms in detail, rather to study their implications for ionospheric flow and auroral signatures. However, it should be noted that recent theories (SOUTHWOOD and KIVELSON, 1990; LEE, 1991) do offer an explanation as to why dynamic pressure changes yield transient disturbances in the auroral ionosphere, as have been found by observations (SIBECK *et al.*, 1989; FARRUGIA *et al.*, 1989) and that OWEN and COWLEY (1991) have presented arguments to the effect that plasma cannot impulsively penetrate through the magnetopause. The theory of reconnection has gained a wide degree of acceptance but ionospheric signatures of transient reconnection (FTEs) have remained very elusive.

It is instructive to consider the direction of motion of events. Figure 6 displays an event in the morning sector (MLT \approx 1000) in which plasma, and the event as a whole, moved eastward. Figure 9, on the other hand, displays an event in the afternoon sector (MLT \approx 1400) in which plasma, and the event as a whole, moved westward. In these two cases, therefore, the plasma motion was sunward, towards noon. This sets tight constraints on the point of impact of any dynamic pressure change, which must have been before 1000 MLT in the first case and after 1400 MLT in the second in order for it to give rise to the observed sunward motions. For the impulsive penetration theory, there are even greater difficulties in explaining why the penetrating anti-sunward moving plasma would begin to move sunward were it able to get onto closed field lines. Any amendment to this theory to

produce such an effect also requires that the penetration take place near dawn and dusk for the two cases discussed above. For magnetic reconnection, the solution is simple in that the sunward motion is produced by the effect of magnetic tension and the B_y component of the IMF, which was indeed negative for the event shown in Fig. 6 and positive for the events shown in Figs 9 and 10.

Resolving FTE effects from those of dynamic pressure changes is difficult, because both are predicted to give twin vortical flow patterns and some level of dynamic pressure variability is always present in the solar wind. LOCKWOOD *et al.* (1990a) have discussed how the plasma flow at the centre of the twin vortex, if that can be defined, offers a method of discriminating between the two effects. For dynamic pressure changes, the central plasma flow will be near to perpendicular to, and generally different in magnitude from, the velocity of the pattern as a whole. Conversely, for an FTE the plasma at the centre of the event will move with the same speed and direction as the event as a whole. In order to test for this difference, it is important to average the plasma flow over the whole central region (the open flux tube of the FTE), so that the 'untwisting' rotation of the tube averages to zero. From this criterion, LOCKWOOD *et al.* (1990a) concluded that the events shown in Fig. 10 were more consistent with the FTE model.

There are a number of problems with a dynamic pressure pulse interpretation of the observed transient auroral/flow burst events. The observed similarity of the directions of event motion and plasma motion within the event is inconsistent with this explanation and the observed similarity of the speeds calls for a highly unlikely coincidence to be consistently repeated [see discussion by LOCKWOOD *et al.* (1990a)]. The inferred occurrence of dynamic pressure pulses is also inconsistent with them acting as triggers for these events. The flow patterns away from the event centre are not as predicted for a dynamic pressure pulse and events drift into the polar cap, whereas pressure pulse effects are expected to move around the polar cap boundary. Motion of auroral forms into the polar cap has been suggested due to waves, set up by a pressure pulse, penetrating into the tail lobe (LUI and SIBBECK, 1991). However, this can only influence the ionospheric flows by increasing the conductivity and hence reducing the flows within the auroral event and increasing them outside the event. This is not what is observed: LOCKWOOD *et al.* (1989a,b, 1990) and SANDHOLT *et al.* (1990) show peak flows are within the 630 nm transient and that flows within the 557.7 nm arc are much faster than outside the auroral event.

On the other hand, the available evidence to date does support the reconnection theory, for a number of reasons. Firstly, the East–West motion of events has always been consistent with the sense of the prevailing B_x component of the IMF. However, it must be noted that this is based on only a few days of optical observations (SANDHOLT, 1988) and even fewer days of combined radar and optical observations (LOCKWOOD *et al.*, 1989a,b, 1990a). Furthermore, the zonal-then-poleward pattern of motion of the events is well explained by the predicted motion of newly opened flux tubes. The occurrence of the limited number of events observed to date shows a repetition rate of about 8 min during continuously southward IMF (very similar to that of magnetopause FTE signatures)—other events follow isolated swings of the IMF to southward. The North–South extents of events (~ 200 km) are consistent with the known $\sim 1 R_E$ extent of magnetopause FTEs in their direction of motion. The East–West dimensions are consistent with extended X-line theories of FTEs. Plasma flows within events are, to within experimental uncertainties, the same as motion of the events as a whole (in both speed and direction)—an important feature of an FTE signature. Event lifetimes are broadly consistent with the period for which newly opened flux tubes are estimated to excite convection, as discussed in the first half of this review (LOCKWOOD *et al.*, 1990a). Lastly, we note that recently ELPHIC *et al.* (1990) have reported that these transient flow burst/auroral events have been observed to occur a few minutes after the conjugate ISEE spacecraft detected FTE signatures.

LOCKWOOD *et al.* (1989a) and SANDHOLT *et al.* (1990) have found some evidence from local magnetometers that the perturbation flows around the events seen by the magnetometers were twin vortical. However, as in Fig. 6, the 'return' flows, outside the central flow burst, were relatively weak. A similar observation was made by LOCKWOOD and SMITH (1989, 1990) for an event seen by the DE-2 spacecraft for which these authors showed that the flows, field-aligned currents, low-energy and energetic electrons, ion dispersion and auroral images were all consistent with an FTE interpretation. This feature can be well explained by the FTE model, once open flux tube shape is properly accounted for. This is demonstrated by Fig. 11. Flow equipotentials (streamlines) are shown for three cases of a moving elliptical flux tube, as predicted by WEI and LEE (1990) and independently by LOCKWOOD *et al.* (1990a). The tube dimensions are typical of those inferred by LOCKWOOD *et al.* (1990a) for the events shown in Fig. 10 and are consistent with the SOUTHWOOD *et al.* (1988)/SCHOLER

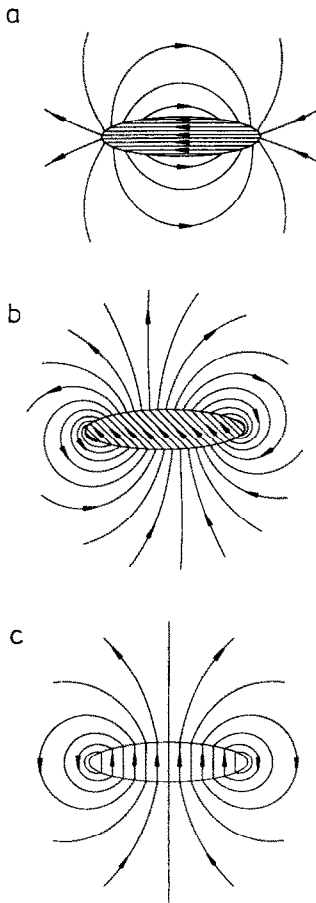


Fig. 11. Flow equipotentials for elliptical FTE flux tubes of major-to-minor axis ratio 4. The major axis is 1000 km in length and is always East–West aligned. The ionospheric conductivities are uniform. In (a) the velocity is westward at 3 km s^{-1} ; in (b) it is North–West at 2 km s^{-1} , and in (c) it is northward at 1 km s^{-1} . The motion of observed optical events typically evolves from that in (a) to that in (c) during their 2–15 min lifetime.

(1988) theory of FTEs being generated by time-varying reconnection at an elongated neutral X -line. The tube is always elongated in the East–West direction [the major-to-minor axis ratio of 4 is also typical of that deduced from all-sky TV images (SANDHOLT, 1988; SANDHOLT *et al.*, 1990) but is not as large as for the event described in Figs 6–8]. The major axis is taken to always be in the East–West direction, as observed in the all-sky images. In part (a) the tube motion is westward at 3 km s^{-1} , in (b) it is north-westward at 2 km s^{-1} and in (c) it is northward at 1 km s^{-1} . This pattern of motion is that described by SANDHOLT *et al.* (1990) for events 1 and 2 in Fig. 10. In the initial phase (a), the event appears as a flow

channel, with only weak return flows outside the region of newly opened flux. In (b) and (c), the twin vortical nature of the flows is more apparent, but because of the large East–West extent of the tube ($\sim 1000 \text{ km}$), the centres of the two vortices are well separated and are unlikely to fall within the field-of-view of any one radar or magnetometer network. The flow pattern (a) is very similar to that observed by the radar in the initial phases of events (e.g. Fig. 6). Patterns like (b) and (c) have not been observed. However, there are a number of good reasons for this. The simplest may be that in phases (b) and (c) the tube is too far to the north of the EISCAT field-of-view. A further complicating assumption is one of the distributions of ionospheric conductivities and their variations with time. This is particularly important when considering the magnetometer signatures which SANDHOLT *et al.* (1990) have shown to be dominated by the strip of highly conducting ionosphere produced by the green line arc. A third important factor is that events rarely occur in isolation, and it is this feature which is discussed further here.

Figure 12 shows schematically the total flow resulting from three elliptical regions of newly opened flux at different phases of their evolution. Note that it is only a sketch, of the kind presented by COWLEY *et al.* (1990), and not a solution of Laplace's equation, with the potential distribution around each event specified by its shape and motion. The pattern of motion of each event is taken from the EISCAT/optical observations and is as expected for newly opened flux tubes (LOCKWOOD and FREEMAN, 1989; SAUNDERS, 1989a,b). A fully consistent model of these flows would need to consider the effect of one region of newly opened flux on the motions of the others. The three events are considered to have been reconnected at the same X -line at intervals of 8 min. The magnetic field topology is taken to be constant so that the ionospheric footprints of each newly opened region first appear at the same MLT (here in the mid-afternoon sector). The regions are elliptical with the same dimensions [East–West (major) axis of 1000 km and North–South axis of 400 km]. These dimensions are typical of those deduced by LOCKWOOD *et al.* (1990a) and are taken not to vary with time (this is an approximation as in general the regions will grow as they propagate, particularly early in their lifetime). Region 3 is the most recently reconnected and is taken to be moving west at 3 km s^{-1} . Region 2 was reconnected 8 min before 3 and is moving northwest at 2 km s^{-1} . The first reconnected region, 1, is moving north at 1 km s^{-1} at the time shown. Hence, if they were present in isolation, regions 1–3 would drive the flows shown in parts (c), (b) and (a), respectively, of Fig.

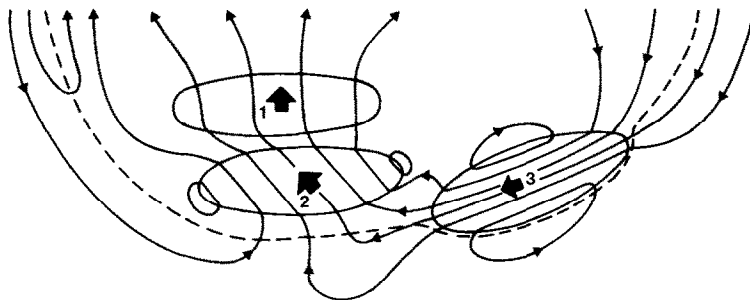


Fig. 12. Schematic of total flow equipotentials for three FTE open flux tubes, reconnected in order 1-3 at 8-min intervals. The event dimensions and motion are as in Fig. 11 (a) (c), respectively. Noon is at the bottom of the figure.

11. The pattern of motion of each event is that observed on 12 January 1988 (SANDHOLT *et al.*, 1990; LOCKWOOD *et al.*, 1989b, 1990a). Some viscous-like interaction across the polar cap boundary (dashed line) has been added near dawn and dusk. Any regions reconnected prior to that labelled 1 are considered not to excite appreciable convection (see previous discussion on the role of open field lines). Figure 12 demonstrates what is possibly the major reason why FTE signatures in the ionosphere have been so hard to detect, namely that the combined effect of a series of elongated events may look very much like a dayside convection pattern. Notice that this concept arises out of the Southwood *et al.*/Scholer model of FTEs which predicts they can be elongated in East-West extent. The flow pattern will vary over an 8-min cycle as new events form and old events cease to excite flows. However, the pattern will maintain the basic characteristics shown in Fig. 12 which are set by the prevailing IMF.

The question arises as to how much of the total transpolar voltage can be attributed to FTEs and the flow pattern sketched in Fig. 12. LOCKWOOD *et al.* (1990a) calculate that, during the period of continuously southward IMF in Fig. 10 (when flow/burst auroral transients occurred roughly every 8 min), that a total of 4.1×10^7 Wb was added to the polar cap in a period of 1350 s, which is a mean voltage of 30 kV. This should be compared with the voltage along the X -lines, which they estimate to vary between 60 and 150 kV (if the reconnection is assumed to proceed for 2 min; if the reconnection burst last longer than this, the reconnection voltage will be correspondingly smaller). For this period, the IMF B_z was roughly -5 nT and the interpolated solar wind speed was $v_{sw} \approx 450$ km s $^{-1}$, giving a motion solar wind electric field of $v_{sw} B_z \approx 2.25$ mV m $^{-1}$. For this value, the scatter plot by COWLEY (1984) yields a total transpolar

voltage estimate in the range 70–130 kV: taking the average value of 100 kV, LOCKWOOD *et al.* (1990a) therefore conclude that FTEs may contribute in the order of 30% to the transpolar voltage during southward IMF. A further 30% (30 kV) could be attributed to viscous-like interactions (as seen when B_z is positive), which leaves 40% (40 kV) which is most easily ascribed to quasi-steady reconnection. In the Southwood *et al.*/Scholer model the latter would occur as a background reconnection rate at the same X -line as produced the FTEs, rather than arise from a second X -line at a different MLT.

8. CONCLUSIONS

High-time resolution studies of dayside ionospheric flows from ground-based radars offer vital new information concerning how convection is excited. The rapid and strong responses of the dayside flows to both northward and southward turnings of the IMF demonstrate that newly reconnected flux tubes are vital for the excitation of dayside convection. As a result, the interplanetary electric field cannot be thought of as mapping down open magnetic field lines into the ionosphere. The temporal evolution of the convection pattern is well explained by the expanding/contracting polar cap model. The ionospheric convection pattern should therefore be thought of as the superposition of two separate patterns with different responses to the IMF. The first pattern is directly driven by solar wind-magnetosphere coupling, dominates the dayside ionospheric flows and is associated with an expanding polar cap area. The second pattern is mainly driven by reconnection in the tail, dominates flows on the nightside and is associated with a contracting polar cap. These two flow patterns can therefore be thought of as the flow

equivalents of the DP-2 and DP-1 current systems, respectively, confirming that current system variability is largely associated with electric field, rather than conductivity, changes.

The dayside cleft/cusp region is found to contain dramatic flow burst events during southward IMF, during which large voltages (often greater than half a typical cross-cap voltage) are found over very small distances. These events are associated with transient auroral displays. Their occurrence and repetition rate is very similar to that of FTEs and their pattern of motion is well explained in terms of newly reconnected

flux tubes. The large East-West extent of the events does support recent theories of FTEs in terms of time-varying reconnection at an elongated reconnection X -line, but uncertainties about field line mapping remain. The large voltages produced across the radar field-of-view by these events (up to 60 kV) indicate that they are a major mechanism for driving convection, indeed a superposition of 2-3 such events in different phases of their evolution may well explain the major features of the pattern of dayside convection and may contribute roughly one-third of the total transpolar voltage.

REFERENCES

- ARNOLDY R. L. 1971 *J. geophys. Res.* **76**, 5189.
 BAKER D. N., HONES E. W. JR, PAYNE J. B. and FELDMAN W. C. 1981 *Geophys. Res. Lett.* **8**, 179.
 BAKER D. N., ZWICKL R. D., BAME S. J., HONES E. W. JR, TSURUTANI B. T., SMITH E. J. and AKASOFU S.-I. 1983 *J. geophys. Res.* **88**, 6230.
 BARGATZE L. F., BAKER D. N., MCPHERRON R. L. and HONES E. W. JR 1985 *J. geophys. Res.* **90**, 6387.
 BERCHEM J. and RUSSELL C. T. 1984 *J. geophys. Res.* **89**, 6689.
 BERING E. A., BENBROOK J. R., BYRNE G. J., LIAO B., THEALL J. R., LANZEROTTI L. J., MACLENNAN C. G., WOLFE A. and SISCOE G. L. 1988 *Geophys. Res. Lett.* **15**, 1545.
 CLAUSER C. R. and KAMIDE Y. 1985 *J. geophys. Res.* **90**, 1343.
 CLAUSER C. R., KELLEY J. D., LOCKWOOD M., ROBINSON R. M., RUOHONIEMI J. M., BEALJARDIERE O. DE LA and HAKKINEN L. 1989 *Adv. Space Res.* **9**(5), 29.
 CLAUSER C. R., MCPHERRON R. L., SEARLES C. and KIVELSON M. G. 1981 *Geophys. Res. Lett.* **8**, 915.
 CORONITI F. V. and KENNEL C. F. 1973 *J. geophys. Res.* **78**, 2837.
 COWLEY S. W. H. 1981 *Planet. Space Sci.* **29**, 79.
 COWLEY S. W. H. 1982 *Rev. Geophys. Space Phys.* **20**, 531.
 COWLEY S. W. H. 1984 *Achievements of the International Magnetospheric Study, IMS. ESA SP-217*, ESTEC, Noordwijk, The Netherlands (p. 483).
 COWLEY S. W. H. 1986 *J. Geomag. Geoelectr.* **38**, 1223.
 COWLEY S. W. H., VAN EYKEN A. P., THOMAS E. C., WILLIAMS P. J. S. and WILLIS D. M. 1990 *J. atmos. terr. Phys.* **52**, 645.
 CROOKER N. U. 1990 *J. geophys. Res.* **95**, 10567.
 CROOKER N. U. and SISCOE G. L. 1990 *J. geophys. Res.* **95**, 3795.
 DESSLER A. J. 1964 *J. geophys. Res.* **69**, 3913.
 ELPHIC R. C. 1988 *Adv. Space Res.* **8**(9), 223.
 ELPHIC R. C., LOCKWOOD M., COWLEY S. W. H. and SANDHOLT P. E. 1990 *Geophys. Res. Lett.* **17**, 2241.
 ETEMADI A., COWLEY S. W. H. and LOCKWOOD M. 1989 *J. atmos. terr. Phys.* **51**, 125.
 ETEMADI A., COWLEY S. W. H., LOCKWOOD M., BROMAGE B. J. I., WILLIS D. M. and LUHR H. 1988 *Planet. Space Sci.* **36**, 471.
 EVANS J. V., HOLT J. M., OLIVER W. L. and WAND R. H. 1983 *J. geophys. Res.* **88**, 7769.
 FARRUGIA C. J., FREEMAN M. P., COWLEY S. W. H., SOUTHWOOD D. J., LOCKWOOD M. and ETEMADI A. 1989 *Planet. Space Sci.* **37**, 589.
 FARRUGIA C. J., RIJNBEEK R. P., SAUNDERS M. A., SOUTHWOOD D. J., RODGERS D. J., SMITH M. F., CHALENOR C. P., HALL D. S., CHRISTENSEN P. J. and WOOLLISCROFT L. J. C. 1988 *J. geophys. Res.* **37**, 14465.

- FRIIS-CHRISTENSEN E., KAMIDE Y., RICHMOND A. D. and MATSUSHITA S. 1985 *J. geophys. Res.* **90**, 1325.
- FRIIS-CHRISTENSEN E., MCHENRY M. A., CLAUER C. R. and VENNERSTRØM S. 1988 *Geophys. Res. Lett.* **15**, 253.
- GLASSMEIER K.-H., HOENISCH M. and UNTIEDT J. 1989 *J. geophys. Res.* **94**, 2520.
- GOERTZ C. K., NEILSEN E., KORTH A., GLASSMEIER K.-H., HALDOUPIS C., HOEG P. and HAYWARD D. 1985 *J. geophys. Res.* **90**, 4096.
- HAPGOOD M. A., BOWE G. A., LOCKWOOD M., WILLIS D. M. and TULUNAY Y. 1991 *Planet. Space Sci.* **39**, 411.
- HEELIS R. A. 1984 *J. geophys. Res.* **89**, 2873.
- HEIKKILA W. J. 1982 *Geophys. Res. Lett.* **9**, 877.
- HEIKKILA W. J., JORGENSEN T. S., LANZEROTTI L. J. and MACLENNAN C. J. 1989 *J. geophys. Res.* **94**, 15291.
- HEPPNER J. P. and MAYNARD N. C. 1987 *J. geophys. Res.* **92**, 203.
- HOLZER T. E., MCPHERRON R. L. and HARDY D. A. 1986 *J. geophys. Res.* **91**, 3287.
- KAMIDE Y., CRAVEN J. D., FRANK L. A., AHN B.-H. and AKASOFU S.-I. 1986 *J. geophys. Res.* **91**, 11235.
- KAMIDE Y. and VICKREY J. F. 1983 *J. geophys. Res.* **88**, 7989.
- LANZEROTTI L. J., HUNSUCKER R. D., RICE D., LEE L. C., WOLFE A., MACLENNAN C. G. and MEDFORD L. V. C. 1987 *J. geophys. Res.* **92**, 7739.
- LANZEROTTI L. J., LEE, L. C., MACLENNAN C. G., WOLFE A. and MEDFORD L. V. C. 1986 *Geophys. Res. Lett.* **13**, 1089.
- LEE, L. C. 1986 *Solar Wind-Magnetosphere Coupling*, KAMIDE Y. and SLAVIN J. A. (eds), p. 297. Terra Scientifica, Tokyo.
- LEE L. C. 1991 *Geophys. Res. Lett.* (in press).
- LEE L. C. and FU Z. F. 1985 *Geophys. Res. Lett.* **12**, 105.
- LEMAIRE J. 1985 *Plasma Phys.* **33-3**, 425.
- LEMAIRE J. and ROTH S. 1978 *J. atmos. terr. Phys.* **40**, 331.
- LOCKWOOD M. and COWLEY S. W. H. 1988 *Adv. Space Res.* **8**(9), 281.
- LOCKWOOD M., COWLEY S. W. H. and FREEMAN M. P. 1990b *J. geophys. Res.* **95**, 7961.
- LOCKWOOD M., COWLEY S. W. H., SANDHOLT P. E. and LEPPING E. D. 1990a *J. geophys. Res.* **95**, 17113.
- LOCKWOOD M., COWLEY S. W. H., TODD, H., WILLIS D. M. and CLAUER C. R. 1988b *Planet. Space Sci.* **36**, 1229.
- LOCKWOOD M., VAN EYKEN A. P., BROMAGE B. J. I., WAITE J. H. JR, MOORE T. E. and DOUPNIK J. R. 1986b *Adv. Space Res.* **6**(3), 93.
- LOCKWOOD M., VAN EYKEN A. P., BROMAGE B. J. I., WILLIS D. M. and COWLEY S. W. H. 1986a *Geophys. Res. Lett.* **13**, 72.
- LOCKWOOD M. and FREEMAN M. P. 1989 *Phil. Trans. Roy. Soc. Lond.* **328A**, 93.
- LOCKWOOD M., SANDHOLT P. E. and COWLEY S. W. H. 1989a *Geophys. Res. Lett.* **16**, 33.
- LOCKWOOD M., SANDHOLT P. E., COWLEY S. W. H. and OGUTI T. 1989b *Planet. Space Sci.* **37**, 1347.
- LOCKWOOD M. and SMITH M. F. 1989 *Geophys. Res. Lett.* **16**, 879.
- LOCKWOOD M. and SMITH M. F. 1990 *Geophys. Res. Lett.* **17**, 305.
- LOCKWOOD M., SMITH M. F., FARRUGIA C. J. and SISCOE G. L. 1988a *J. geophys. Res.* **93**, 5641.
- LUI A. T. Y. and SIBECK D. G. 1991 *J. atmos. terr. Phys.* **53**, 219.
- LUNDIN R. 1988 *Space Sci. Rev.* **48**, 263.
- LYONS L. R. 1985 *J. geophys. Res.* **90**, 1561.
- MCHENRY M. A. and CLAUER C. J. 1987 *J. geophys. Res.* **92**, 11231.
- MCPHERRON R. L. and MANKA R. H. 1985 *J. geophys. Res.* **90**, 1175.
- NISHIDA A. 1968a *J. geophys. Res.* **73**, 5549.
- NISHIDA A. 1968b *J. geophys. Res.* **73**, 1795.
- NISHIDA A. and KAMIDE Y. 1983 *J. geophys. Res.* **88**, 7005.
- OGUTI T., YAMAMOTO T., HAYASHI K., KOKUBUN S., EGELAND A. and HOLTET J. A. 1988 *J. Geomag. Geoelectr.* **40**, 387.
- OWEN C. J. and COWLEY S. W. H. 1991 *J. geophys. Res.* (in press).
- PASCHMANN G., HAERENDEL G., PAPAMASTORAKIS I., SCKOPKE N., BAME S. J., GOSLING J. T. and RUSSELL C. T. 1982 *J. geophys. Res.* **87**, 2159.
- PASCHMANN G., PAPAMASTORAKIS I., BAUMJOHANN W., SCKOPKE N., CARLSON C. W., SONNERUP B. U. O. and LÜHR H. 1986 *J. geophys. Res.* **91**, 11099.

- PELLINEN R. J., BAUMJOHANN W., HEIKKILA W. J.,
SERGEEV V. A., YAHNIN A. G., MARKLUND G.
and MELNIKOV A. O. 1982 *Planet. Space Sci.* **30**, 217.
- REIFF P. H. and LUHMANN J. G. 1986 *Solar Wind-Magnetosphere Coupling*, KAMIDE Y. and
SLAVIN J. A. (eds), p. 453. Terra Scientifica, Tokyo.
- REIFF P. H., SPIRO R. W., WOLF R. A., KAMIDE Y.
and KING J. H. 1985 *J. geophys. Res.* **90**, 1318.
- RICHMOND A. D., KAMIDE Y., AHN B.-H.,
AKASOFU S.-I., ALCAYDE D., BLANC M.,
BEAUJARDIERE O. DE LA, EVANS D. S., FOSTER J. C.,
FRIIS-CHRISTENSEN E., FULLER-ROWELL T. J.,
HOLT J. M., KNIPP D., KROEHL H. W.,
LEEPING R. P., PELLINEN R. J., SENIOR C.
and ZAITZEV A. N. 1988 *J. geophys. Res.* **93**, 5760.
- RUNBEEK R. P., COWLEY S. W. H., SOUTHWOOD D. J.
and RUSSELL C. T. 1984 *J. geophys. Res.* **89**, 786.
- RISHBETH H., SMITH P. R., COWLEY S. W. H.,
WILLIS D. M., EYKEN A. P. VAN, BROMAGE B. J. I.
and CROTHERS S. R. 1985 *Nature* **318**, 451.
- ROBINSON R. M., CLAUSER C. R.,
BEAUJARDIERE O. DE LA, KELLEY J. D.,
FRIIS-CHRISTENSEN E. and LOCKWOOD M. 1989 *J. atmos. terr. Phys.* **52**, 411.
- ROSTOKER G., SAVOIE D. and PHAN T. D. 1988 *J. geophys. Res.* **93**, 8633.
- RUSSELL C. T. 1972 The configuration of the magnetosphere. In *Critical
Problems of Magnetospheric Physics*, DYER E. R.
(ed), p. 1. IUCSTP Secretariat, National Academy
of Sciences, Washington, U.S.A.
- RUSSELL C. T. and ELPHIC R. C. 1978 *Space Sci. Rev.* **22**, 681.
- RUSSELL C. T. and ELPHIC R. C. 1979 *Geophys. Res. Lett.* **6**, 33.
- RYCROFT M. J. 1987 *Mem. Natl Inst. Polar Res.* **48**, 196.
- SANDHOLT P. E. 1988 *Adv. Space Res.* **8**(9), 21.
- SANDHOLT P. E., EGELAND A., HOLTET J. A.,
LYBEKK B., SVENES K. and ASHEIM S. 1985 *J. geophys. Res.* **90**, 4407.
- SANDHOLT P. E., LOCKWOOD M., OGUTI T.,
COWLEY S. W. H., FREEMAN K. S. C., EGELAND A.,
LYBEKK B. and WILLIS D. M. 1990 *J. geophys. Res.* **95**, 1039.
- SANDHOLT P. E., JACOBSON B., LYBEKK B.,
EGELAND A., BYTHROW P. F. and HARDY D. A. 1989b *J. geophys. Res.* **94**, 6317.
- SANDHOLT P. E., LYBEKK B., EGELAND A.,
NAKAMURA R. and OGUTI T. 1989a *J. Geomag. Geoelectr.* **41**, 371.
- SAUNDERS M. A. 1989a *Geophys. Res. Lett.* **16**, 151.
- SAUNDERS M. A. 1989b *Antarctic Sci.* **1**, 193.
- SAUNDERS M. A., RUSSELL C. T. and SCKOPKE N. 1984 *Magnetic Reconnection in Space and Laboratory
Plasmas*, HONES E. W. Jr. (ed.), p. 145. AGU Mono-
graph 80, AGU, Washington, D.C.
- SCHATTEN K. H. and WILCOX J. W. 1967 *J. geophys. Res.* **72**, 5185.
- SCHOLER M. 1988 *Geophys. Res. Lett.* **15**, 291.
- SCHUNK R. W. and RAITT W. J. 1980 *J. geophys. Res.* **85**, 1255.
- SERGEEV V. A., DMITRIEVA N. P.
and BARKOVA E. S. 1986 *Planet. Space Sci.* **34**, 1109.
- SIBECK D. G., BAUMJOHANN W. and LOPEZ R. E. 1989 *Geophys. Res. Lett.* **16**, 13.
- SISCOE G. L. and HUANG T. S. 1985 *J. geophys. Res.* **90**, 543.
- SOUTHWOOD D. J. 1985 *Adv. Space Res.* **5**(4), 7.
- SOUTHWOOD D. J. 1987 *J. geophys. Res.* **92**, 3207.
- SOUTHWOOD D. J., FARRUGIA C. J.
and SAUNDERS M. A. 1988 *Planet. Space Sci.* **36**, 503.
- SOUTHWOOD D. J. and KIVELSON M. G. 1990 *J. geophys. Res.* **95**, 2301.
- STERN D. P. 1973 *J. geophys. Res.* **78**, 7292.
- ST-MAURICE J.-P. and HANSON W. B. 1982 *J. geophys. Res.* **87**, 7580.
- TODD H., BROMAGE B. J. I., COWLEY S. W. H.,
LOCKWOOD M., VAN EYKEN A. P. and
WILLIS D. M. 1986 *Geophys. Res. Lett.* **13**, 909.
- TODD H., COWLEY S. W. H., BROMAGE B. J. I.,
ETEMADI A., LOCKWOOD M., WILLIS D. M.
and LÜHR H. 1988a *J. atmos. terr. Phys.* **50**, 423.

- TODD H., COWLEY S. W. H., BROMAGE B. J. I.,
ETEMADI A., LOCKWOOD M., WILLIS D. M.
and LÜHR H. 1988b *Planet. Space Sci.* **36**, 1415.
- TOFFOLETTO F. R. and HILL T. W. 1989 *J. geophys. Res.* **94**, 329.
- VAN EYKEN A. P., RISHBETH H., WILLIS D. M.
and COWLEY S. W. H. 1984 *J. atmos. terr. Phys.* **46**, 635.
- WEI C. Q. and LEE L. C. 1990 *J. geophys. Res.* **95**, 2405.
- WILLIS D. M., LOCKWOOD M., COWLEY S. W. H.,
VAN EYKEN A. P., BROMAGE B. J. I., RISHBETH H.,
SMITH P. R. and CROTHERS S. R. 1986 *J. atmos. terr. Phys.* **48**, 987.
- WRIGHT A. W. 1987 *Planet. Space Sci.* **35**, 813.